Analyzing The Effects of Various Factors on Emission During Combustion of N-Dodecane In Gas Turbine Engine

Saravanan.R[1], Periyasamy.S[2]
[1] Dept of Mechanical Engineering
[2]Assistant Professor, Dept of Mechanical Engineering
[1, 2] Government College of Technology, Coimbatore, India

Abstract- *Nowadays air transports have been increasing rapidly. As a result, the emission of toxic gases from the aircraft engines is also increasing very rapidly which affect the atmosphere. Governments of various countries are producing stringent rules regarding the emission of toxic gases such as NOX and carbon dioxide and carbon monoxide. Nitrous oxides were formed as as secondary products of complete combustion. Carbon monoxide is formed as a result of incomplete combustion. The production of these toxic gases depends on various parameters in which adiabatic flame temperature plays a major role.*

The adiabatic flame temperature of combustion in aircraft engines depends on various parameters which includes height above the sea level, pressure ratio, inlet or initial temperature which also depends on on the pressure ratio and also on the equivalence ratio. Here the effects of these parameters on the adiabatic flame temperature of n-dodecane are analyzed and compared with the experimental results.

I. INTRODUCTION

Engineering determining methods:

Engineers have always been interested in understanding and predicting the behaviour of fluid flow system behaviour & variables. There are three way of predicting methods which are included below:

- Experimental Method
- Analytical / Mathematical Methods
- Numerical Methods

Experimental method:

The most reliable and easiest way to predict the natural phenomenon is usually done by gathering the information about the measurements. This is the common way of gathering the information of the full scale equipment and predicts how the equipment would behave in real life application.

This method of using or actually collecting the information can result time loss as rigorous experiments needs to be conducted to find the minute changes. Application: In small scale product development, in using the past data for future design and development. Examples include: Aero planes.

Analytical method:

This method works on the consequences of the mathematical model. These mathematical models describe the behaviour of the system. Usually the mathematical model is a set of differential equations which are used to solve the problem.

Numerical method:

It finds the behaviour of the physical properties on the product using set of defined differential equations by means of digital computing. It uses the physical properties of the product from the experimental data and pre-defined set of differential equations to understand the behaviours and effects. It breaks the problem into discrete parts where it uses set of equations on each discrete part. Numerical method can be classified into three categories of discretization methods to understand the meshing:

- Finite Difference Method:
- Finite Element Method:
- Finite Volume Method:

Computational Fluid Dynamics:

Introduction To CFD:

Fluids (gasses and liquid) are governed by partial equations that represent the general laws of conservation of mass, momentum and energy. CFD is the art of replacing such PDE by set of equations which can be solved by the digital computers. Computational Fluid Dynamics (CFD) provides quantitative and qualitative predictions of the fluid flow by means of the following:

- Modeling by applications of mathematics of partial differential equations
- Use of discretion and solution tools i.e. numerical methods.
- Use of the software tools like solvers, pre and post processing utilities.

CFD is essential software which enables the engineers to virtually simulate the numerical experiments carried in the laboratories resulting in less time consuming process and better accurate results. CFD gives an insight to the pattern of the fluid flow that is difficult to predict with regular experiments, expensive to conduct and sometimes impossible to study by the regular experiments.

Factors Of CFD

The CFD software use mathematical tools to solve the problem which is a pre-set of equations. The main factor of CFD is

- The researcher who feeds the problem into the computer
- Scientific knowledge that is expressed mathematically.
- The computer code that consists of the algorithms that embodies the knowledge
- Hardware of the computer that performs the calculations
- The researcher who simulates and interprets the data. CFD is a highly disciplinary subject that indulges into the research area and lies at the interface of physics, applied mathematics and computer science.

CFD ANALYSIS PROCESS

CFD analysis process can be summarized in the following steps:

1. Problem Statement:
2. Mathematical Model:
3. Discretization Process
4. CFD Simulation
5. Post Processing and Analysis
6. Uncertainty and errors
7. Validation of the CFD models. .
8. Validation of CFD Codes

Meshing :

Usually the discretion process converts every continuous system to a discrete one. This means that the grids or the mesh generation is done to obtain the approximate solution at each discrete grid. Grid generation of mesh is either of the two types.

1. Structured Mesh generation
2. Unstructured mesh generation

These four different methods follow a basic set of rules mentioned below:

1. Generation of the valid mesh. This means that the mesh should have no holes or self-intersection.
2. Conformation of the mesh with the boundary.
3. Balancing the density of the mesh to control the accuracy and computational requirements.

The popular methods to generate finite volume meshing in CFD are:

1. Surface Meshing
2. Advancing front method
3. Delaunay triangulation method

Application in the research methodology:

Automatic unstructured meshing has been used in the mesh generation. However the mesh sizes have been defined to as low values approx. – 1 mm to 2 mm to increase the mesh quantity and quality for better accuracy in results.

Mesh Quality

Mesh quality plays a crucial role in the determination of the accuracy of the results, irrespective of the types of mesh being used.

1. Mesh Element Distribution:

It is important to have a fine mesh element distribution. Since the domain is discretely defined, the salient features of the fluid flow depend on the mesh density and distribution. The mesh distribution in the research is fine and uniform.

2. Cell Quality:

It depends on the skewness and aspect ratio. Skewness is defined as the difference between the shape of the cell and shape of the equilateral cell of equivalent volume while aspect ratio is the measure of stretching the cell. In a general rule for a good mesh is to have the triangular mesh with skewness less than 0.95

Boundary Conditions :

Boundary conditions serve the important and most required conditions for the mathematical model . These direct the motion flow of the fluid in the domain. They are also defined as the face zone in CFD. Application in the research: There has been significant use of the boundary conditions in the research. Inlet & Outlet Boundary: The inlet & outlet boundary is the condition which serves as the input and output or inlet & outlet of the fluid flow in the domain. They can be of different types, such as:

- For incompressible flows: Velocity inlet and outflow.
- General: Pressure inlet and outlet.
- For compressible flow: Mass inlet and outlet
- Special cases: Inlet and outlet vent.

Most of the time, the selection of the inlet and outlet depends on the type of geometry.

Computing setup:

Parallel computing for processing has been used in the processing set up for the models. The reason of using parallel computing is because; single processing allows solving one discrete problem at one time. Parallel processing is used to make more than one processing at a time. This is time efficient while double precision is used to change the magnitude order of the residuals.

CONVERGENCE:

Convergence is the way of obtaining accuracy. All the models in the research work have been converged before they are proceeded to post processing analysis. Convergence is the way of obtaining accuracy for the model. Number of iterations is made to run to check the convergence of the governing equations. This is usually estimated by the RMS value depending on the precision of the processor (either single or double). RMS value usually varies between 106 to 1012 . Once the convergence is achieved, the results can be more precise. Application in the research work: Every model before post processing in the ANSYS Fluent is checked for convergence. This is obtained by the successfully running the iterations along with the equations. The solutions once converged results in better accuracy of the results.

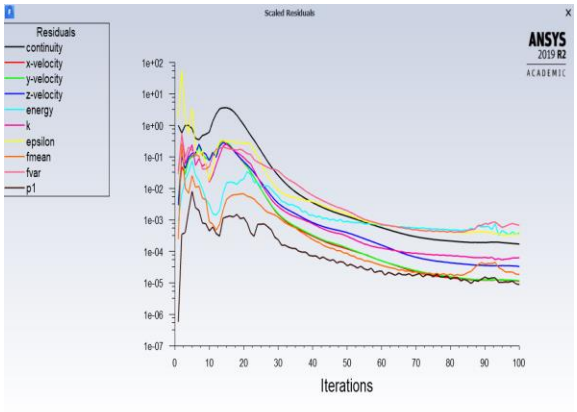

FIG: 1 Convergence Of A Problem

Errors:

- Physical Errors
- Discretization Error
- Truncation Error
- Computer-round off Error
- Iterative Convergence Error

II. GAS TURBINE ENGINES

In gas turbine engines, various types of fuels such as Jet-A and Jet-B type of fuels are being used. We are taking Jet – A type of fuel in our project.

Jet-A Fuel:

A successful modeling of combustion and emissions of gas turbine engine combustors requires an adequate description of the reaction mechanism. For hydrocarbon oxidation, detailed mechanisms are only available for the simplest types such as methane, ethane, acetylene, ethylene, and propane. 1,2 These detailed mechanisms contain a large number of chemical species participating simultaneously in many elementary kinetic steps. Current computational fluid dynamics (CFD) models involve chemical reactions, turbulent mixing, fuel vaporization, and complicated boundary geometries, etc.

To simulate these conditions requires a sophisticated computer code, which usually requires a large memory capacity an take a longtime to simulate. To get around these problems, the gas turbine combustion modeling effort has frequently been simplified by using a global approach that reduces chemistry to the specification of an overall global reaction mechanisms, which can predict quantities of interest:

heat release rates, flame temperature, emissions, and ignition delay time.

The simplest Jet-A reaction mechanism is the one-step mechanism:

$$C_nH_m+(n+m/2)\ 0_2 \rightarrow nCO_2 + m/2\ H_2O \quad ..(1)$$

where the coefficients n, m are the carbon to hydrogen ratio. The advantage of this mechanism is its simplicity; it involves the solution of the conservation equations for unburned fuel and mixture fraction, the heat release and other species concentrations are obtained from linear functions of the amount of fuel consumed. This mechanism, however, fail to predict the important characteristics of Jet-A oxidation, i.e., the formation of intermediates and CO. As a result, this mechanism is over predict the heat of reaction, hence higher adiabatic flame temperatures.

A slightly more complex mechanism is the two-step mechanism proposed by Edelman and Fortune:3

$$C_nH_m+(n/2+m/4)\ O_2 \rightarrow nCO + m/2\ H_2O \quad ..(2)$$

$$CO + 20_2 \rightarrow 4\ CO_2 \quad ..(3)$$

This involves one global reaction describe the formation of CO and H_2O, and a second global reaction describe the formation of CO_2 . However the formation of intermediates is still ignored and so this mechanism cannot predict the time delay between the initial disappearance of fuel into intermediates and a significant rise in temperature.

The objective of this study is to define a mechanism that can explain most of the observed phenomena in our flame tube experiment. The proposed mechanism involves 16 species and 21 elementary reactions. The initial breakdown of the fuel molecule has been assumed to be the reaction of the fuel molecule with oxygen; the chain carriers are CH_2, 0 and OH radicals, assumed Jet-A structure is $C_{13}H_{27}$: Initiation:

$$C_{13}H_{27} + 0_2 \rightarrow 13CH_2 + H0_2 \quad ..(4)$$

These important steps in the chain propagation are:

$$CH_2 + 0_2 \rightarrow CH_20 + 0 \quad ..(5)$$

$$M + CH_2O \rightarrow CO + H_2 \quad ..(6)$$

$$0 + H_2 \rightarrow OH + H \quad ..(7)$$

The species CH_2 has been considered here as a representative of unburned hydrocarbon fragments.

The importance of this species increases with increase in fuel concentration. The above reaction steps have been combined with the existing mechanism of hydrogen—air oxidation reported by Nguyen and Bittker, 4 some reaction rates were replaced by more recent values reported by Miller. 5 The activation energy used for Jet-A oxidation was close to the value reported by Freeman. 6

The proposed mechanism was first examined through a sensitivity analysis with the use of in-house Sensitivity Analysis Program Code, the orders of importance for the species of interest and classification of reactions in descending order of importance are determined. The resulting mechanism was then validated by calculated ignition delay time with experimental ignition delay time. Then using this mechanism to calculate results from plug flow reactor code were verified with in-house experimental flame tube data.

III. LITERATURE SURVEY

Importantly, many investigators have found that reaction mechanisms originally developed for air-combustion may produce questionable results under oxy-fuel conditions (Andersen et al., 2009; Bibrzycki and Poinsot, 2010).

Clifford A. Moses and his colleague performed a research to identify the tests and presents the results demonstrating that Sasol fully synthetic jet fuel (FSJF) is fit-for-purpose as jet fuel for civilian aviation. The FSJF is the synthetic fuel produced by combining many processes which include F-T process. The main idea of FSJF process is producing a fully synthetic jet fuel which contains aromatic fraction. Aromatic fraction in Jet fuel plays a role in some fuel properties of jet fuel such as, improving cold flow properties, density, low heating value by volume and cause swelling in rubber and certain sealants [35]… With the aim that satisfies all the property requirements of international specifications for jet fuel, four samples blends ware developed, covering the practical range of production. Chemistry and physical properties and characteristics were tested to demonstrate that Sasol FSJF will be typical of conventional jet fuel. Furthermore, the combustion characteristics, emissions, engine durability, and performance were evaluated on a series of engine and combustor tests as a final demonstration. The results showed that the performance of the synthetic test fuel was typical of conventional jet fuel.

PremLobo performed a study on measurements of particulate master (PM) emissions from a CFM56-7B commercial jet engine fueled conventional (Jet A1) and alternative biomass based and FT-based fuels. The results of experiment showed

that there was reduction of PM emissions for using biomass and FT-based fuels compared with those of using Jet A1.

Edwin Corporan studied on the emissions characteristics of two combustion platforms, a T63 turbo shaft engine and an atmospheric swirl-stabilized research combustor, fueled with conventional military jet fuel (JP-8), a natural gas derived F-T synthetic jet fuel, and blends of the two were investigated. The results show that there are dramatic reductions in particle concentration and mean size on both combustion platforms with neat F-T and blends relative to operation with JP-8. Using neat F-T fuel decreases 80% in smoke number, sulfur oxide emissions, while slightly increase in water vapor compared to operation on JP-8. The tests results also find that JP-8/FT synthetic jet fuel blends up to 50/50% by volume satisfied the standard requirements of JP-8, and if at higher F-T synthetic jet fuel concentrations, only minimum specific gravity requirement was not satisfied the standard.

chi-ming lee and Krishna kundu(1991), Lewis Research Center, Cleveland, Ohio did a study for Jet-A Reaction mechanism study for combustion application and found that the adiabatic flame temperature to occur between 1889k and 2069 k for equivalence ratios of 0.471 to 0.588.

Glarborg and Bentzen (2008) found that, relative to combustion in air, more CO is produced during oxy-fuel combustion via reactions of CO_2 with H_2 and CH_x radicals. Andersen et al. (2009)discovered that the CO formation during oxy-fuel combustion is overestimated by the global reaction mechanisms originally developed for traditional methane air-combustion.

Leiser et al. (2007); **Bibrzyckiand Poinsot** (2010**); Hjärtstam et al.** (2012); Yin et al. (2011) and Hu et al.(2018) also pointed out that the reaction mechanisms for air-combustion may not accurately predict results of oxy-fuel combustion. Therefore, it is highly necessary to evaluate the performance of reaction mechanisms under oxy-fuel conditions. To the best of our knowledge, no detailed mechanisms have been comprehensively tested in oxy-fuel combustion.

For instance, the well known GRI-Mech 3.0 (**Smith et al.,** 1999) and USC-Mech II (**Wang et al**.,2007) mechanisms were originally developed for combustion in air, and their performance for oxy-fuel combustion is still unknown. Moreover, although the detailed mechanism of Peter Glarborg's group (Mendiaraand Glarborg, 2009b) was specifically developed for oxy-fuel conditions(their mechanism is termed OFD in the present study), this mechanism has not been systematically validated with a large set of oxy-fuel experiments. The present study will first evaluate the predictions of several detailed Mechanisms under oxy-fuel conditions. However, just evaluating mechanism does not guarantee its suitability for practical use. The use of computational fluid dynamics modeling with detailed mechanisms to model realistic combustor requires significant computing resources(Edge et al., 2011; Hu et al., 2018),

Especially for large eddy simulation(LES) (Pitsch, 2006) and direct numerical simulation (DNS). Although the computational cost can be significantly reduced by using a two-step or four-step global mechanism, the global mechanism cannot precisely capture transient processes and limit behaviors such as ignition and extinction because of the failure for build-up of the radical pool(**Andersen et al.,** 2009; Hu et al., 2018). To maintain the accuracy of a mechanism while simultaneously decreasing the calculation cost, it is essential to develop simplified mechanisms based on a well-evaluated detailed mechanism. Therefore, after mechanism evaluation, the present study will then develop a new reduced mechanism for oxy-fuel combustion that involves minimal species and reactions, and more importantly, does not significantly decrease the accuracy. For small hydrocarbon fuels, the mechanism reduction process involves two main steps: skeletal simplification and time-scale analysis (Lu and Law, 2009). For the first step, unimportant species and reactions are eliminated (Niemeyer et al., 2010). These unimportant species and reactions are identified and removed by a variety of systematic methods, including sensitivity analysis, Jacobian analysis (Turányiand Tomlin, 2014), CSP (Lam, 1993; Valorani et al., 2006

.

Combustion and emission Characteristics in a can – type combustion chamber by **selvakumar kumaresh, Man Young Kim**, International journal of mechanical and mechatronics Engineering, Volume 8, Number:7, 2014 deals with the combustion characteristics such as swirl ratio, inlet temperature , pressure in the emission characteristics.

Additionally, skeletal mechanisms can be obtained by the CSP method with fast and slow importance indices (Lam, 1993; Lu and Law, 2006b; **Valorani et al**., 2006).

IV. METHODOLOGY

The experiment can be started with the help of designing the combustion chamber, setting the input parameters such height, pressure ratio amount of mass flow rate inside the combustion chamber and then followed by the analysis in fluent and finally post processing.

Formulae used:

The formulae used for the calculation of mass flow rate and the number of injectors for the given mass flow rate is given below

$$mass\ flow\ rate = \frac{power}{Lower\ Heating\ Value}$$

$$Mass\ flow\ rate\ of\ injectors = \frac{total\ mass\ flow\ rate\ of\ fuel}{number\ of\ fuel\ injectors}$$

$$Total\ mass\ flow\ rate\ of\ air = \frac{mass\ flow\ rate\ of\ fuel * 100}{5.5}$$

Assuming 5.5 % of fuel

$$Mass\ flow\ rate\ of\ pimary\ air = Total\ mass\ flow\ rate\ of\ air * 0.75$$

$$Mass\ flow\ rate\ of\ secondary\ air = \frac{total\ mass\ flow\ rate\ of\ air * 0.25}{number\ of\ air\ injectors}$$

Drawing The Model In Solid works:

In this stage, a simplified scale down model of can type combustion chamber is drawn using SOLIDWORKS.

Importing Of Geometry In Ansys Fluent:

The geometry of scale down model of can type combustion geometry is imported into the ANSYS FLUENT. The part should be saved in IGS format so that it can open.

Meshing:

In meshing part, first the surfaces of the model were given name so that the model can be analyzed easily during the process.

Surfaces of primary air supply, secondary air supply, fuel injectors and outlet were created.

The curvature part of the model should be meshed finely.

Element size were set to 30 mm.

Set up:

- Energy equation is set to ON.
- K-Ɛ was chosen for viscous equation
- P1 radiation model was chosen
- Non – pre mixed combustion was preferred.
- Species was chosen correctly.
- Boundary conditions were provided.
- Initialization was done appropriately.

Calculations:

Once the calculate button is clicked, the computer do the calculations and finishes every step. If the meshing elements were high, then sometimes it can take more than 20 hours for a single calculation.

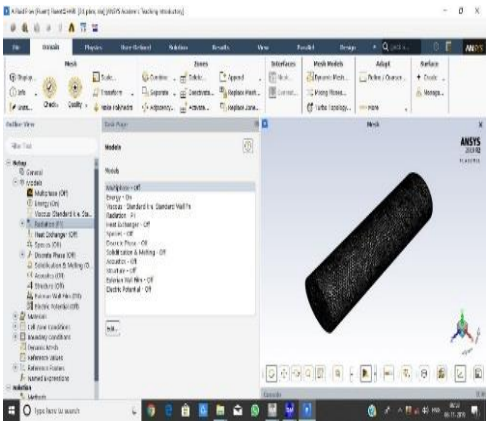

FIG: 2 Input Geometry

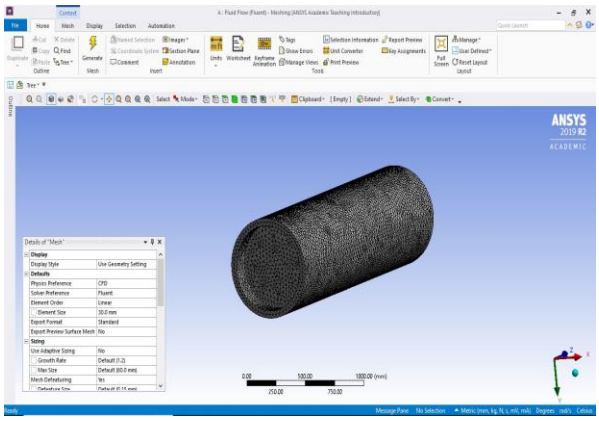

FIG: 3 Meshing

Sizing → curvature → off

Element Size → 30 mm

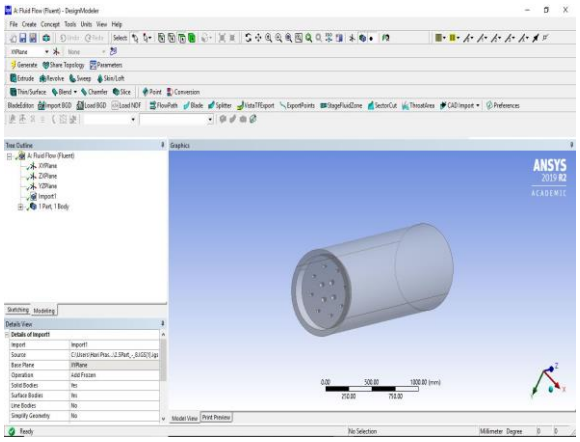

FIG: 4 Set Up

Energy Equations	-	ON
Viscous Equation	-	K – Ɛ
Radiation Model	-	P1
Species	-	Jet A
Input type	-	Mass flow rate

V. RESULTS AND DISCUSSION

Contours:

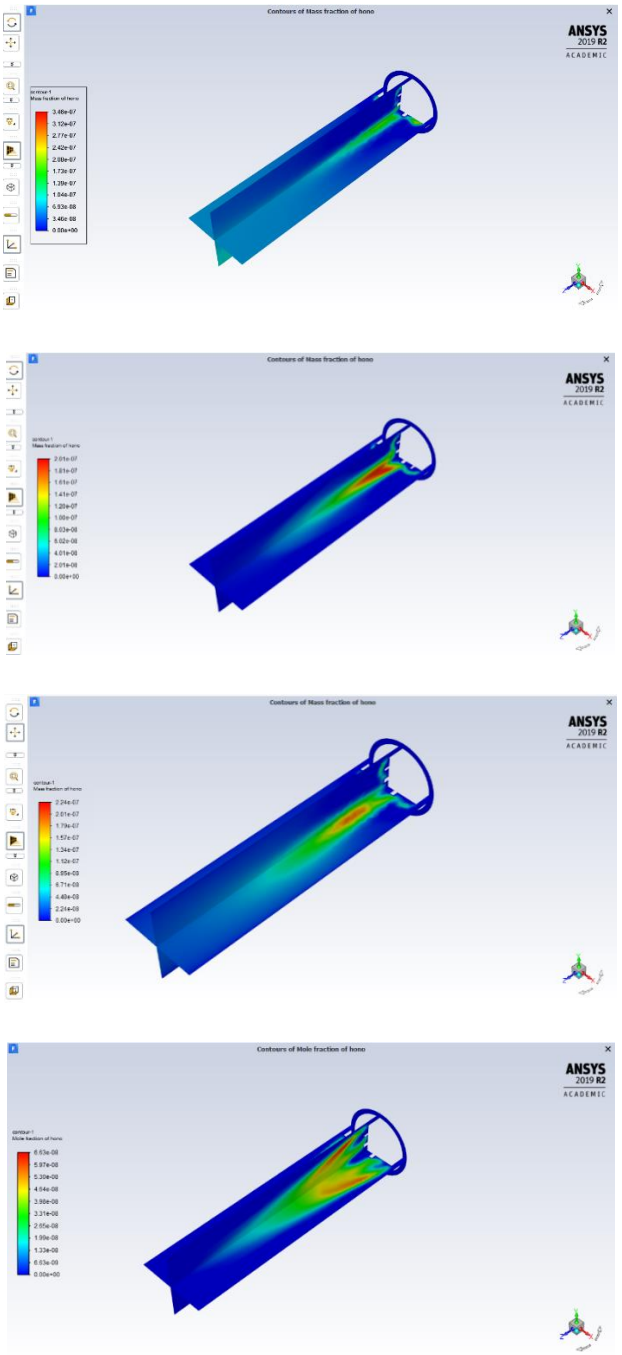

FIG 5 Amount Of Nitrous Oxides Formed During Combustion

As the mass flow rate increases, the amount of nitrous oxides produced inside the combustion chamber increases. But also it decreases as the number of injectors increased for the same mass flow rate.

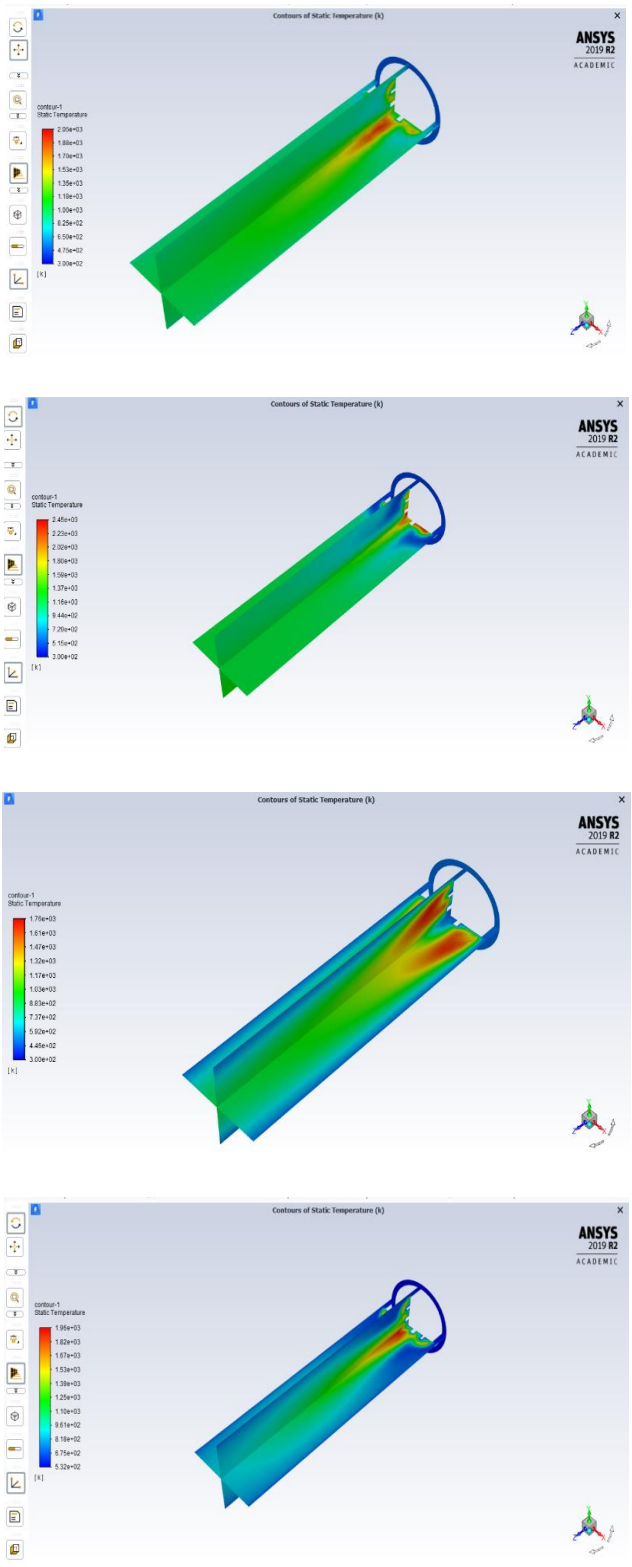

FIG 6 Temperature Profile

The adiabatic flame temperature starts decreasing as the number of injectors are increased for the same amount of mass flow rate of fuel.

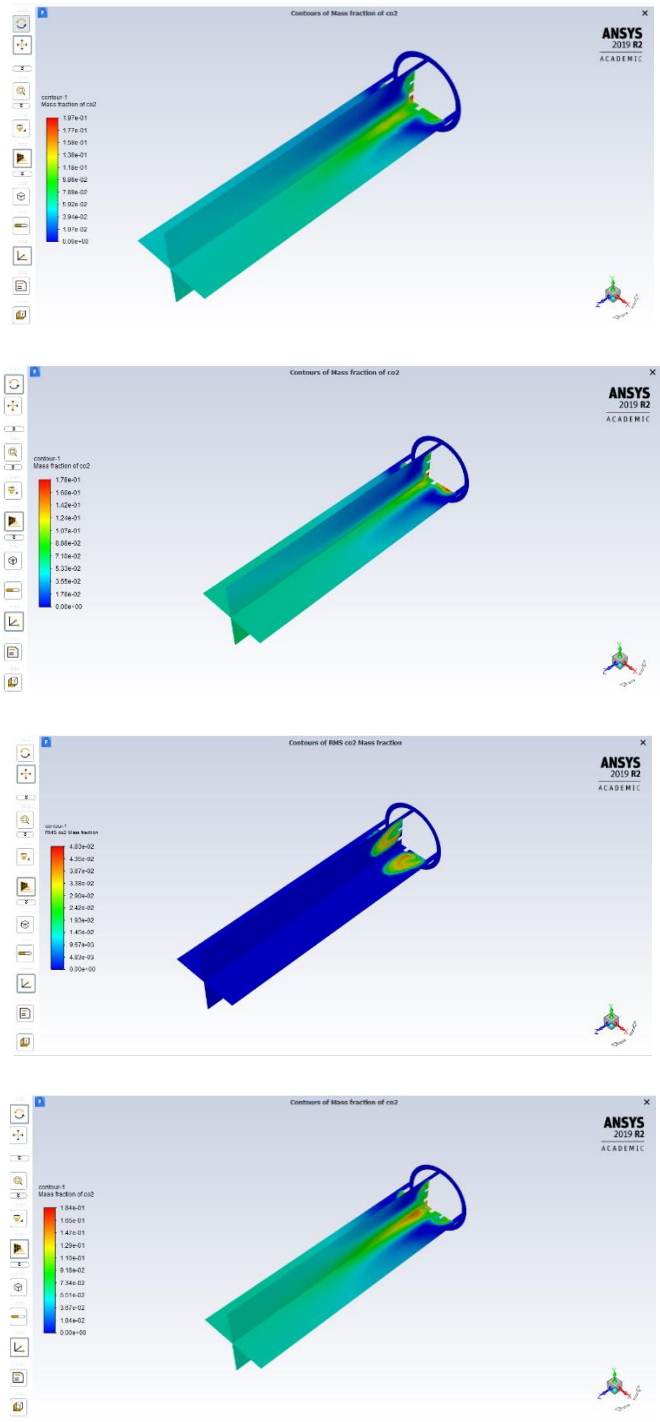

FIG 7 Co_2 Profile

Carbon di oxide is produced as the result of complete combustion. Less amount of carbon dioxide near the injectors represent the incomplete combustion. For this problem swirl injectors can be designed and then studied which leads to in-depth study.

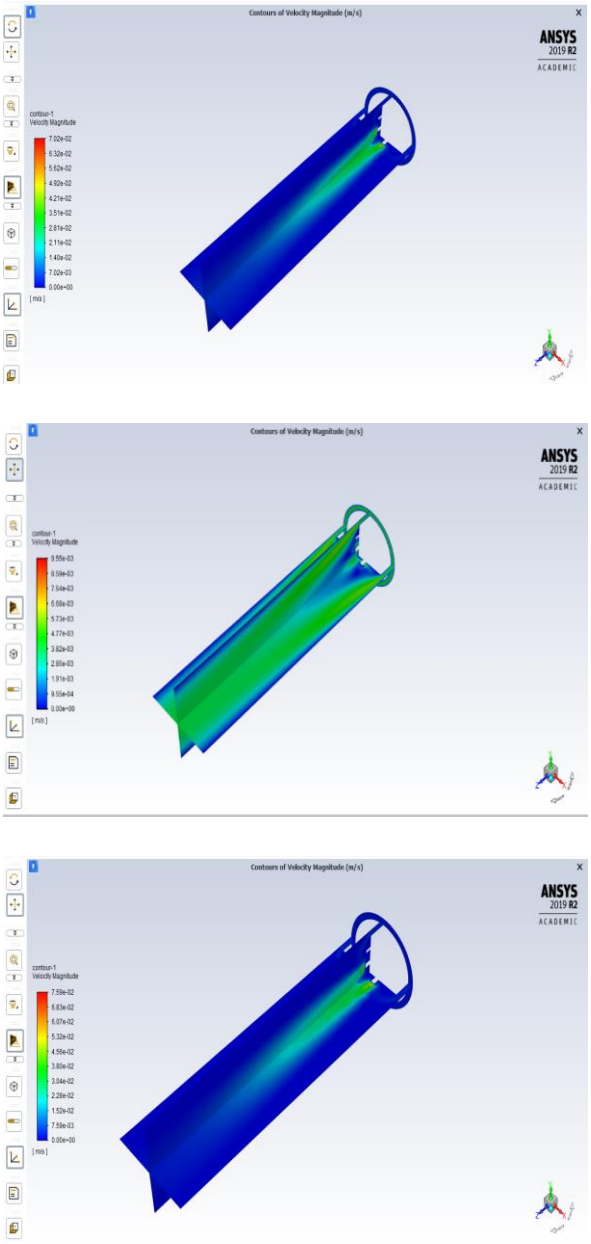

FIG 8 Velocity Profile

More the amount of mass flow rate of fuel, more will be the velocity. Less amount of mass flow rate of fuel leads to unburnt fuel. An optimum amount of mass flow rate of fuel should be used for proper mixing of air and fuel which leads to efficient combustion.

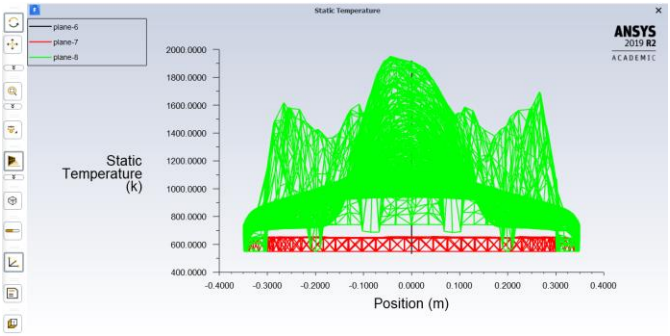

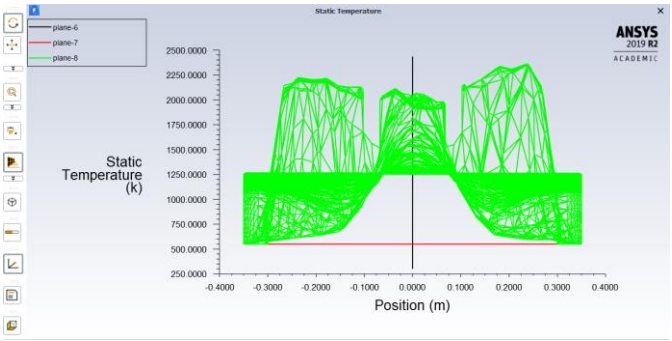

FIG 9 Maximum Temperature

Maximum adiabatic flame temperature corresponds to the production of nitrous oxides. S it should be avoided.

Analysis Of n-Dodecane Combustion

Adiabatic Flame Temperature:

The adiabatic flame temperature for various initial condition are given below in the following tables 1, 2, 3.

Table 1: Adiabatic Flame Temperature For varying heights and r_p= 18

INLET TEMPERATURE (K)		538.97	531.54	524.12	516.70	509.28	501.85	494.43
INLET PESSURE(Pa)		640057.59	595045.06	552631.09	512699.32	475137.02	439835.08	406687.92
HEIGHT (m)		8000	8500	9000	9500	10000	10500	11500
		ADIABATIC FLAME TEMPERATURE (K)						
EQUIVALENCE RATIO	0.1	811.2	804.2	797.2	790.3	783.3	776.3	769.3
	0.2	1059.6	1053.0	1046.4	1039.7	1033.1	1026.5	1019.9
	0.3	1290.4	1283.9	1277.5	1271.1	1264.7	1258.3	1252.0
	0.4	1506.7	1500.4	1494.2	1488.0	1481.8	1475.5	1469.3
	0.5	1710.2	1704.1	1698.0	1692.0	1685.9	1679.8	1673.8
	0.6	1901.5	1895.5	1889.6	1883.6	1877.7	1871.8	1865.9
	0.7	2079.4	2073.5	2067.7	2061.9	2056.0	2050.2	2044.4
	0.8	2239.5	2233.7	2227.9	2222.2	2216.4	2210.6	2204.8
	0.9	2372.3	2366.4	2360.5	2354.6	2348.7	2342.8	2336.9
	1	2457.8	2451.7	2445.7	2439.6	2433.5	2427.4	2421.3
	1.1	2460.5	2454.6	2448.7	2442.7	2436.7	2430.8	2424.8
	1.2	2397.0	2391.2	2385.4	2379.6	2373.8	2368.0	2362.3
	1.3	2319.7	2313.9	2308.1	2302.4	2296.6	2290.9	2285.2
	1.4	2242.1	2236.3	2230.6	2224.9	2219.1	2213.4	2207.7
	1.5	2166.5	2160.7	2155.0	2149.3	2143.5	2137.8	2132.1
	1.6	2093.2	2087.4	2081.7	2075.9	2070.2	2064.5	2058.8
	1.7	2022.1	2016.4	2010.6	2004.9	1999.1	1993.4	1987.7
	1.8	1953.2	1947.4	1941.6	1935.9	1930.1	1924.4	1918.7
	1.9	1886.2	1880.4	1874.6	1868.8	1863.1	1857.4	1851.7
	2	1821.0	1815.2	1809.4	1803.6	1797.9	1792.1	1786.4
	2.1	1757.5	1751.7	1745.9	1740.1	1734.3	1728.6	1722.8
	2.2	1695.6	1689.7	1683.9	1678.1	1672.3	1666.6	1660.8
	2.3	1635.1	1629.3	1623.4	1617.6	1611.8	1606.1	1600.3
	2.4	1576.1	1570.2	1564.4	1558.5	1552.7	1546.9	1541.1
	2.5	1518.3	1512.4	1506.6	1500.7	1494.9	1489.0	1483.2
	2.6	1461.8	1455.9	1450.0	1444.1	1438.3	1432.4	1426.6
	2.7	1406.7	1400.7	1394.7	1388.8	1382.9	1377.0	1371.1
	2.8	1353.4	1347.3	1341.3	1335.3	1329.3	1323.3	1317.3
	2.9	1304.7	1298.5	1292.2	1286.0	1279.8	1273.6	1267.5
	3	1267.8	1261.3	1254.8	1248.3	1241.8	1235.4	1228.9

As the altitude increases, the pressure decreases, which leads to lower inlet temperature. This will lead to lower adiabatic flame temperature at high altitudes for the same pressure ratio but at the cost of reduced power.

Table 2: Adiabatic Flame Temperature For Low Pressure Ratio

INLET TEMPERATURE K		509.3	517.2	524.8	532.2
INLET PRESSURE Pa		475137.0	501533.5	527930.0	554326.5
PRESSURE RATIO		18	19	20	21
		ADIABATIC FLAME TEMPERATURE K			
EQUIVALENCE RATIO	0.1	783.28	790.75	797.94	804.88
	0.2	1033.10	1040.19	1047.01	1053.60
	0.3	1264.74	1271.58	1278.18	1284.55
	0.4	1481.76	1488.41	1494.83	1501.03
	0.5	1685.88	1692.37	1698.63	1704.68
	0.6	1877.70	1884.03	1890.14	1896.04
	0.7	2056.03	2062.18	2068.11	2073.84
	0.8	2216.38	2222.33	2228.07	2233.61
	0.9	2348.74	2354.51	2360.07	2365.43
	1	2433.49	2439.19	2444.67	2449.96
	1.1	2436.73	2442.56	2448.17	2453.59
	1.2	2373.82	2379.80	2385.56	2391.13
	1.3	2296.64	2302.67	2308.49	2314.12
	1.4	2219.13	2225.19	2231.04	2236.70
	1.5	2143.54	2149.62	2155.49	2161.16
	1.6	2070.23	2076.32	2082.20	2087.90
	1.7	1999.14	2005.25	2011.15	2016.86
	1.8	1930.15	1936.27	1942.19	1947.91
	1.9	1863.10	1869.24	1875.17	1880.91
	2	1797.86	1804.01	1809.96	1815.71
	2.1	1734.31	1740.48	1746.44	1752.21
	2.2	1672.33	1678.52	1684.50	1690.29
	2.3	1611.83	1618.03	1624.03	1629.84
	2.4	1552.70	1558.93	1564.95	1570.78
	2.5	1494.87	1501.12	1507.16	1513.01
	2.6	1438.25	1444.53	1450.60	1456.47
	2.7	1382.90	1389.21	1395.31	1401.21
	2.8	1329.28	1335.63	1341.76	1347.70
	2.9	1279.80	1286.16	1292.31	1298.26
	3	1241.85	1248.13	1254.19	1260.05

For compression pressure ratios from 18 to 21 the inlet temperature vary from 509 to 532 k and the adiabatic flame temperature vary from 1797 to 1851 k for equivalence ratio 2.

Table 3: Adiabatic Flame Temperature For Medium Pressure Ratio

INLET TEMPERATURE K		539.3	546.2	552.9	559.4	565.7
INLET PRESSURE Pa		580723.0	607119.5	633516.0	659912.5	686309.0
PRESSURE RATIO		22	23	24	25	26
		ADIABATIC FLAME TEMPERATURE K				
EQUIVALENCE RATIO	0.1	811.58	818.07	824.36	830.47	836.40
	0.2	1059.98	1066.15	1072.14	1077.96	1083.61
	0.3	1290.72	1296.69	1302.49	1308.12	1313.60
	0.4	1507.03	1512.84	1518.48	1523.96	1529.30
	0.5	1710.54	1716.21	1721.72	1727.07	1732.28
	0.6	1901.75	1907.28	1912.65	1917.87	1922.95
	0.7	2079.38	2084.76	2089.98	2095.05	2099.98
	0.8	2238.96	2244.16	2249.19	2254.09	2258.85
	0.9	2370.62	2375.64	2380.50	2385.23	2389.82
	1	2455.07	2460.01	2464.79	2469.43	2473.94
	1.1	2458.83	2463.89	2468.81	2473.58	2478.22
	1.2	2396.52	2401.74	2406.82	2411.75	2416.55
	1.3	2319.58	2324.86	2330.00	2335.00	2339.86
	1.4	2242.18	2247.50	2252.67	2257.69	2262.59
	1.5	2166.67	2172.01	2177.19	2182.24	2187.16
	1.6	2093.42	2098.77	2103.98	2109.04	2113.97
	1.7	2022.39	2027.77	2032.99	2038.06	2043.01
	1.8	1953.46	1958.85	1964.08	1969.18	1974.14
	1.9	1886.47	1891.87	1897.12	1902.23	1907.21
	2	1821.29	1826.71	1831.98	1837.10	1842.09
	2.1	1757.80	1763.24	1768.52	1773.66	1778.67
	2.2	1695.90	1701.35	1706.65	1711.80	1716.83
	2.3	1635.47	1640.94	1646.25	1651.43	1656.47
	2.4	1576.43	1581.91	1587.25	1592.44	1597.50
	2.5	1518.68	1524.19	1529.54	1534.76	1539.84
	2.6	1462.17	1467.70	1473.08	1478.32	1483.43
	2.7	1406.94	1412.50	1417.91	1423.18	1428.31
	2.8	1353.46	1359.05	1364.49	1369.78	1374.94
	2.9	1304.02	1309.62	1315.06	1320.35	1325.51
	3	1265.73	1271.24	1276.60	1281.81	1286.88

From pressure ratio 22 to 26, the inlet temperature vary from 539 to 565k. The adiabatic flame temperature vary from 1821 to 1842 k for equivalence ratio 2.

Table 4: Adiabatic Flame Temperature For High Pressure Ratio

INLET TEMPERATURE K		571.8	577.8	583.6	589.3
INLET PRESSURE Pa		712705.5	739102.0	765498.5	791895.0
PRESSURE RATIO		27	28	29	30
		ADIABATIC FLAME TEMPERATURE K			
EQUIVALENCE RATIO	0.1	842.17	847.78	853.26	858.60
	0.2	1089.12	1094.48	1099.72	1104.83
	0.3	1318.93	1324.13	1329.20	1334.15
	0.4	1534.49	1539.56	1544.50	1549.32
	0.5	1737.35	1742.30	1747.12	1751.84
	0.6	1927.90	1932.73	1937.44	1942.04
	0.7	2104.79	2109.47	2114.04	2118.51
	0.8	2263.48	2268.00	2272.41	2276.71
	0.9	2394.29	2398.64	2402.88	2407.02
	1	2478.32	2482.59	2486.75	2490.80
	1.1	2482.73	2487.13	2491.42	2495.60
	1.2	2421.22	2425.78	2430.23	2434.57
	1.3	2344.60	2349.22	2353.73	2358.14
	1.4	2267.36	2272.01	2276.56	2281.00
	1.5	2191.95	2196.62	2201.19	2205.65
	1.6	2118.78	2123.48	2128.06	2132.54
	1.7	2047.84	2052.55	2057.15	2061.64
	1.8	1978.98	1983.70	1988.32	1992.83
	1.9	1912.07	1916.81	1921.44	1925.96
	2	1846.96	1851.72	1856.37	1860.91
	2.1	1783.56	1788.33	1792.99	1797.55
	2.2	1721.73	1726.52	1731.20	1735.77
	2.3	1661.39	1666.19	1670.89	1675.48
	2.4	1602.44	1607.26	1611.97	1616.58
	2.5	1544.80	1549.64	1554.37	1559.00
	2.6	1488.41	1493.27	1498.03	1502.68
	2.7	1433.32	1438.21	1442.98	1447.66
	2.8	1379.97	1384.89	1389.69	1394.38
	2.9	1330.54	1335.45	1340.25	1344.94
	3	1291.82	1296.65	1301.36	1305.97

All the above values show that the adiabatic flame temperature increases with input temperature, but at the same time it increases with the equivalence ratio up to 1 and then decreases.

The Adiabatic flame temperature is plotted in the graph against the equivalence ratio for the graphical representation of variations in adiabatic flame temperature

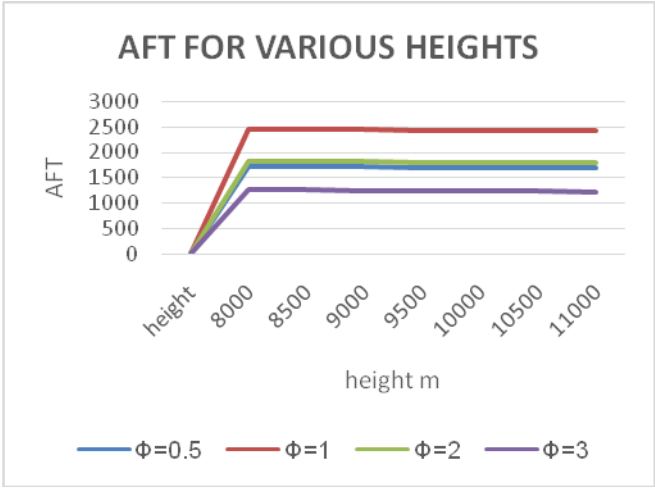

Graph 1: Adiabatic Flame Temperature Vs Equivalence Ratio For Various Heights

From the Graph 1 it show that the adiabatic flame temperature varies with equivalence ratio in a parabolic manner that show that it attains only high temperature at equivalence ratio 1 and consistently increasing for the increasing initial temperature. Also the initial combustion temperature decreases with increase in height.

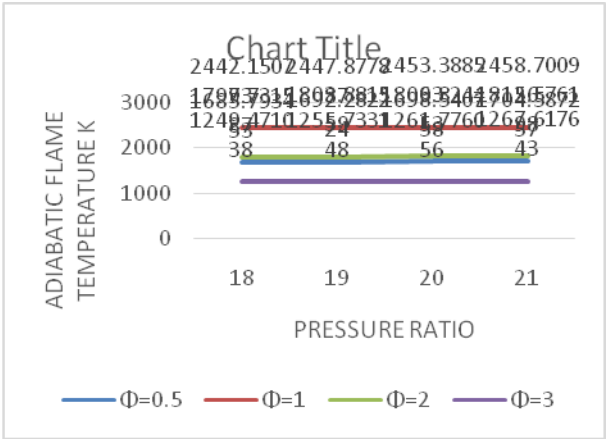

Graph 2: Adiabatic Flame Temperature Vs Equivalence RatioFor Low Pressure Ratios

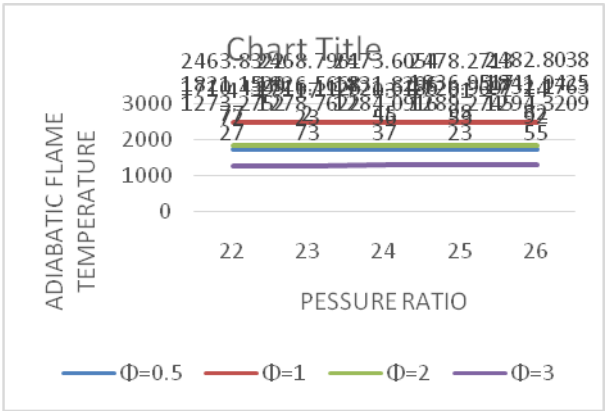

Graph 3: Adiabatic Flame Temperature Vs Equivalence Ratio For Medium Pressure Ratios

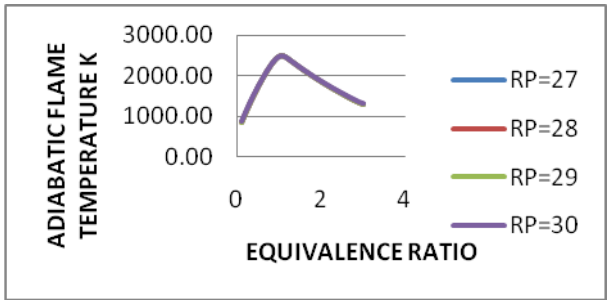

Graph 4: Adiabatic Flame Temperature Vs Equivalence Ratio For High Pressure Ratios

From the Graph 2, 3, 4 it shows that the adiabatic flame temperature varies with equivalence ratio in a parabolic manner that show that it attains only high temperature at equivalence ratio 1 and consistently increasing for the increasing initial temperature. Also as the pressure ratio increases the temperature after the compression process also increases which leads to increase in combustion inlet temperature.

VI. CONCLUSION

Gas turbine engines were mainly used in aircrafts which operates at various altitudes and at various compression ratios which changes the combustion environment. As the inlet or initial temperature increases, the adiabatic flame temperature also increases, which is the same case as the change in pressure ratio. As the height increases, the temperature of the atmosphere decreases, which leads to decrease in combustion inlet temperature and results in the decrease of adiabatic flame temperature. However at certain altitudes mass flow rate of air inside the engine will be low. So we have to adjust with low propulsive power. For that an optimum value of altitude10000 m and the equivalence ratio 0is chosen. For this given value the adiabatic flame temperature varies in the range of 1850 to2000 k.

Further, the adiabatic flame temperature can be reduced by considering the effects of swirl which will be continued in the second phase on different geometries. Once we are able to decrease the maximum adiabatic flame temperature, we can also subsequently reduce the nitrous oxide emissions.

REFERENCES

[1] Jet-A Reaction mechanism study for combustion application by chi-ming lee and Krishna kundu, Lewis Research Center, Cleveland, Ohio
[2] Aviation Fuels Overview by Gozdem Kilaz, School of Engineering Technology.
[3] Oxy-Fuel Combustion Modeling: Performance of Global Reaction Mechanisms Stefan Hjärtstam,* Fredrik Normann, Klas Andersson, and FilipJohnsson
[4] A Minimal Skeletal Mechanism for Combustion of CH4/O2/CO2 mixtures Xianzhong Hu, Qingbo Yu, Yanming Li, and Junxiang Liu
[5] Measurement of propagation speeds in adiabatic cellular premixed flames of CH4 + O2 + CO2 Alexander A. Konnov *, Igor V. Dyakov
[6] Using CSP to Understand Complex Chemical KineticsS. H. Lama
[7] Experimental and kinetic studies of ignition processes of the methane–nheptane mixtures Junjie Lianga, Zunhua Zhanga, GeshengLia, Qi Wanb, Li Xub, ShidongFanb
[8] Skeletal mechanism generation for surrogate fuels using directed relation graph with error propagation and sensitivity analysis Kyle E. Niemeyer [a], Chih-Jen Sung [b], Mandhapati P. Raju[c]
[9] Development of an Experimental Database and Chemical Kinetic Models for Surrogate Gasoline Fuels W. J. Pitz
[10] Progress in Chemical Kinetic Modeling for Surrogate Fuels W. J. Pitz, C. K. Westbrook, O. Herbinet, E. J.Silke
[11] Evaluation, development, and validation of a new reduced mechanism for Methane oxy-fuel combustion Fan Hu, Pengfei Li, JunjunGuo, Kai Wang, Zhaohui Liu, Chuguang Zheng